LETTER

doi:10.1038/nature12971

DNA-guided DNA interference by a prokaryotic Argonaute

Daan C. Swarts[1]*, Matthijs M. Jore[1]*, Edze R. Westra[1], Yifan Zhu[1], Jorijn H. Janssen[1], Ambrosius P. Snijders[2], Yanli Wang[3], Dinshaw J. Patel[4], José Berenguer[5], Stan J. J. Brouns[1] & John van der Oost[1]

RNA interference is widely distributed in eukaryotes and has a variety of functions, including antiviral defence and gene regulation[1,2]. All RNA interference pathways use small single-stranded RNA (ssRNA) molecules that guide proteins of the Argonaute (Ago) family to complementary ssRNA targets: RNA-guided RNA interference[1,2]. The role of prokaryotic Ago variants has remained elusive, although bioinformatics analysis has suggested their involvement in host defence[3]. Here we demonstrate that Ago of the bacterium *Thermus thermophilus* (TtAgo) acts as a barrier for the uptake and propagation of foreign DNA. *In vivo,* TtAgo is loaded with 5′-phosphorylated DNA guides, 13–25 nucleotides in length, that are mostly plasmid derived and have a strong bias for a 5′-end deoxycytidine. These small interfering DNAs guide TtAgo to cleave complementary DNA strands. Hence, despite structural homology to its eukaryotic counterparts, TtAgo functions in host defence by DNA-guided DNA interference.

To elucidate the physiological role of Ago in prokaryotes, we studied Ago from *T. thermophilus*. Comparison of the *ago* genes of the type strain HB27 (refs 4, 5) and a derivative with enhanced competence (HB27^{EC}; Fig. 1a and Extended Data Fig. 1a), revealed that an insertion sequence (IS*Tth7*)[6] disrupts *ago* in HB27^{EC}. In line with a role of TtAgo in reducing competence, a generated Δ*ago* mutant (HB27Δ*ago*; Fig. 1a) has a natural transformation efficiency that is a factor of ten higher than the wild-type HB27 ($P < 0.02$, Fig. 1b). Complementation of the knockout strain with *ago* (HB27Δ*ago*::^{s}*ago* (HB27Δ*ago* complemented with a *strep(II)-tag-ago* gene fusion insert); Fig. 1a, b) almost completely restores the wild-type phenotype. Moreover, isolation of plasmid and total DNA from the wild-type and the *ago* knockout strains revealed lower plasmid yields from the wild-type strain, indicating that TtAgo reduces the intracellular plasmid concentration ($P < 0.02$, Fig. 1c; $P < 0.02$, Fig. 1d).

We performed transcriptome analysis of HB27 and HB27Δ*ago* to determine whether TtAgo-mediated interference proceeds directly by targeting plasmid DNA, or indirectly by regulating gene expression. Although the comparison revealed pleiotropic changes in gene expression (Extended Data Fig. 2), we did not observe substantial differential expression of genes involved in plasmid uptake or host defence (Extended Data Table 1). Hence, RNA sequencing (RNA-seq) analysis suggests that TtAgo does not influence plasmid uptake and plasmid copy number at the level of transcriptional control.

We therefore studied whether TtAgo interacts with plasmid DNA. In agreement with the RNA-seq analysis (Extended Data Fig. 2), affinity-purified TtAgo expressed from the chromosome of HB27Δ*ago*::^{s}*ago* could be detected by protein mass spectrometry (Extended Data Table 2). Unfortunately, molecular analysis of TtAgo expressed in *T. thermophilus* was hampered by the low TtAgo yield, and attempts to overexpress TtAgo in *T. thermophilus* from a plasmid were unsuccessful. By contrast, expression of Strep(II)-tagged TtAgo (Fig. 2a) in *Escherichia coli* was successful when performed at 20 °C. Under these conditions, TtAgo has no effect on plasmid content (Extended Data Fig. 1b). Analysis of co-purified nucleic acids revealed that TtAgo-associated RNA (10–150 nucleotides) is preferentially ^{32}P-labelled in a polynucleotide kinase

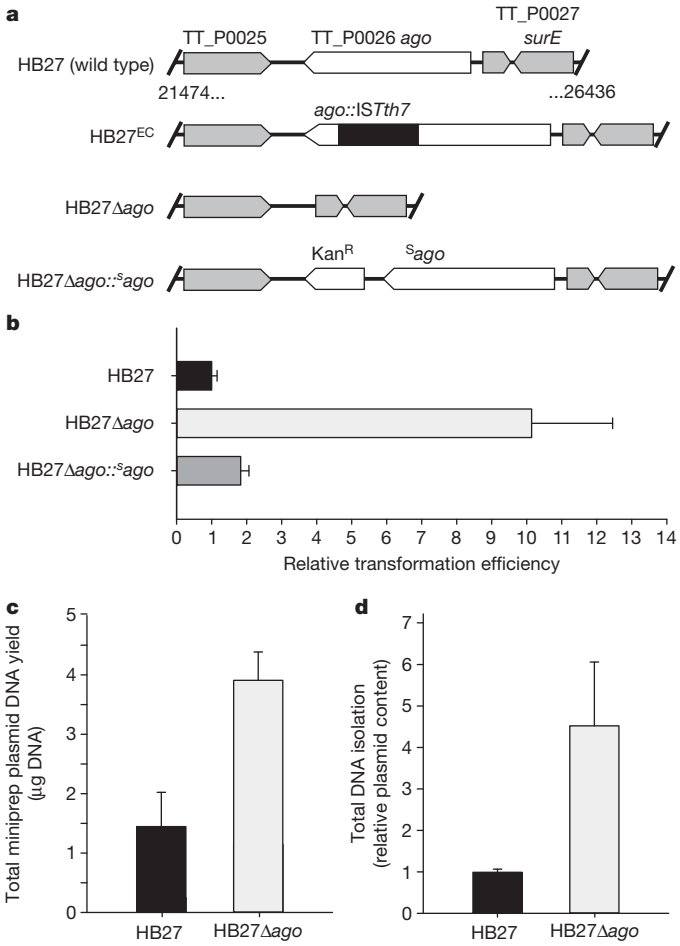

Figure 1 | TtAgo interferes with plasmid DNA. a, Overview of *ago* gene loci of *T. thermophilus* strains: HB27 (wild type), HB27^{EC} (spontaneous derivative with enhanced competence), HB27Δ*ago* (knockout), and HB27Δ*ago*::^{s}*ago* (HB27Δ*ago* complemented with a *strep(II)-tag-ago* gene fusion insert). Kan^{R}, kanamycin resistance marker. **b**, Transformation efficiency of *T. thermophilus* strains on transformation with the plasmid pMHPnqosGFP (Extended Data Table 5). Error bars indicate standard deviations of biological duplicates. **c**, Yield of pMHPnqosGFP plasmid mini preparation (miniprep) of HB27 and HB27Δ*ago*. Error bars indicate standard deviations of biological triplicates. **d**, Plasmid content of total DNA purified from HB27Δ*ago* relative to that from HB27, as quantified by Genetools (Syngene) after resolving the DNA on a 0.8% agarose gel. Error bars indicate standard deviations of biological triplicates.

[1]Laboratory of Microbiology, Department of Agrotechnology and Food Sciences, Wageningen University, Dreijenplein 10, 6703 HB Wageningen, the Netherlands. [2]Clare Hall Laboratories, Cancer Research UK, London Research Institute, South Mimms EN6 3LD, UK. [3]Institute of Biophysics, Chinese Academy of Sciences, Beijing 100101, China. [4]Structural Biology Program, Memorial Sloan-Kettering Cancer Center, New York, New York 10065, USA. [5]Centro de Biología Molecular Severo Ochoa, UAM-CSIC, Campus de Cantoblanco, 28049 Madrid, Spain.
*These authors contributed equally to this work.

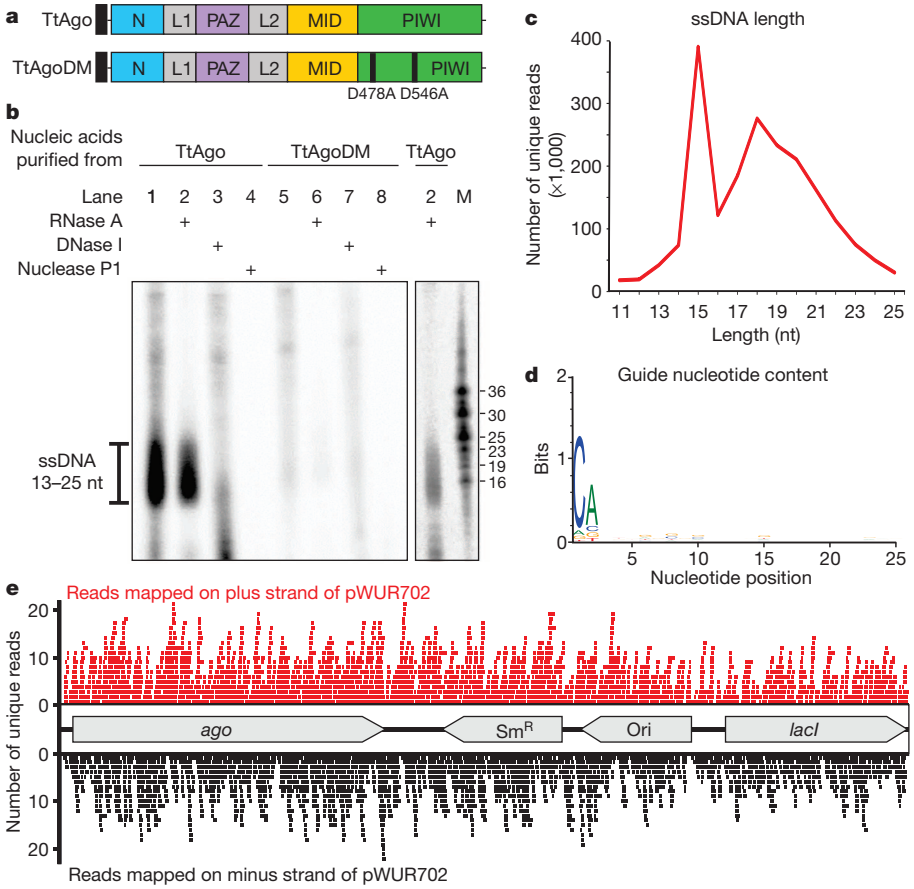

Figure 2 | TtAgo guides are 5′-phosphorylated DNA molecules. **a**, Schematic representation of TtAgo and TtAgoDM proteins used for all experiments (N, PAZ, MID, and PIWI are structural domains, L1 and L2 are linkers[8]). The amino-terminal Strep(II)-tag is indicated as a black square. **b**, Co-purified nucleic acids from TtAgo and TtAgoDM are labelled with [γ-^{32}P]ATP after phosphate exchange by PNK from bacteriophage T4, and treated with enzymes as indicated. M, custom ssDNA marker; nt, nucleotides. **c**, Length distribution of unique ssDNA sequences co-purified with TtAgo. **d**, Nucleotide composition of unique ssDNA sequences co-purified with TtAgo. **e**, Unique reads of TtAgo co-purified ssDNA molecules mapped on the TtAgo expression vector pWUR702.

(PNK) forward reaction, indicating the presence of 5′ hydroxyl groups (Extended Data Fig. 1c). By contrast, co-purified DNA has a more defined length (13–25 nucleotides), and is preferentially labelled in a PNK exchange reaction, indicating phosphorylated 5′ ends (Fig. 2b). A 5′ phosphate group is a general feature of Ago guides[7–11].

Whereas eukaryotic Ago proteins exclusively use ssRNA guides, some prokaryotic Ago proteins have a higher affinity for single-stranded DNA (ssDNA) guides[9,10]. Moreover, the characteristics of the small DNAs that associate with TtAgo *in vivo* are in agreement with previously described *in vitro* guide requirements[8,12,13]. TtAgo catalyses cleavage of ssDNA targets *in vitro* when supplied with complementary 5′-phosphorylated 21-nucleotide ssDNA guides, but not when supplied with analogous ssRNA guides[8,12,13] (Extended Data Fig. 3). During isolation of an active site double mutant, TtAgoDM (TtAgo(D478A,D546A); Fig. 2a), only RNAs co-purify (10–150 nucleotides; Extended Data Fig. 1c). This suggests that active site residues are involved in processing and/or binding of the ssDNA molecules.

Cloning and sequencing of TtAgo-bound DNA molecules resulted in 70.6 million sequences, of which 65% can be mapped on the TtAgo expression plasmid pWUR702, 3% on the plasmid pRARE, and 32% on the chromosome of *E. coli* K12 (Extended Data Table 3). Remarkably, when normalized for the DNA content in each cell, TtAgo predominantly co-purifies with guides complementary to pWUR702 and pRARE (approximately 54 and 8.8 times more frequently, respectively), rather than with guides complementary to the *E. coli* K12 chromosome (Extended Data Table 3).

More detailed analysis of unique guide sequences revealed two populations of DNA guides: one 15-nucleotides long, and the other ranging from 13 to 25 nucleotides in length (Fig. 2c). No obvious bias towards specific regions of the plasmids or the chromosome was detected: the guides target coding and non-coding regions on both strands independent of GC content (Fig. 2e). Some guides map on one of the plasmids as well as on the chromosome of *E. coli* (for example, on *lacI* and *proL*). The fact that these guides do not seem to be under-represented compared with other plasmid-targeting guides indicates that there is no selection against chromosome-targeting guides, but rather that the differential guide loading (Extended Data Table 3) is a result of preferential acquisition of guides from plasmids.

Interestingly, 89% of the DNA guides have a deoxycytidine (dC) at the first position at the 5′ end and 72% have a deoxyadenosine (dA) at the second position (Fig. 2d). Despite this bias, identical TtAgo cleavage activities are observed with DNA guides containing a 5′ dC, dT, dA or dG (Extended Data Fig. 4a–d). The 5′ dC preference may result from specific guide processing, or from preferential 5′ nucleoside selection by TtAgo. A bias for specific 5′ nucleosides also occurs in certain eukaryotic Ago proteins[14,15].

We performed activity assays to investigate whether the *in vivo* plasmid-derived ssDNAs are functional guides that enable TtAgo to cleave double-stranded DNA (dsDNA) targets (expression plasmid pWUR702). Purified TtAgo linearizes or nicks pWUR702, resulting in linear or open circular plasmid DNA, respectively (Fig. 3a, lane 4), whereas TtAgoDM does not show this activity (Fig. 3a, lane 3). The cleavage activity of TtAgo is strongly temperature dependent: whereas ssDNA is cleaved at temperatures ≥20 °C, plasmid DNA is only cleaved at temperatures ≥65 °C (Extended Data Fig. 4e, f). This agrees with the observation that during TtAgo expression in *E. coli* at 20 °C, plasmid concentrations are not decreased (Extended Data Fig. 1b). Purified TtAgo is unable to cleave plasmids that have no sequence similarity to pWUR702 or pRARE (for example, pWUR708; Fig. 3b, lane 4). However, when supplied with two synthetic 5′-phosphorylated ssDNA guides that target both strands of the plasmid at the same locus (Fig. 4b), TtAgo was able to linearize or nick pWUR708 (Fig. 3b, lane 8). These findings, together with the guide sequence data, indicate that the *in vivo* acquired DNA molecules guide TtAgo to cleave dsDNA targets. We

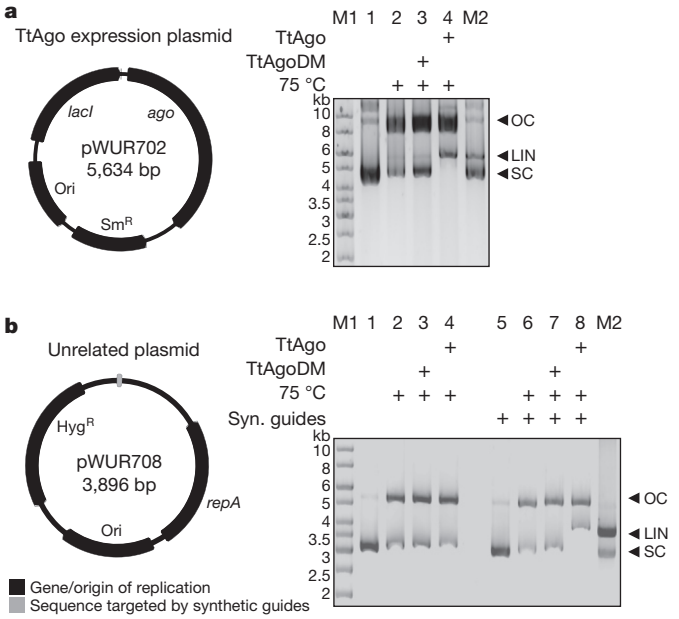

Figure 3 | TtAgo cleaves plasmids complementary to its guides. **a**, **b**, Untreated target plasmid (lane 1, 5), plasmid incubated at 75 °C in the absence of proteins (lane 2, 6), or in the presence of TtAgoDM (lane 3, 7) or TtAgo (lane 4, 8) purified from *E. coli*, resolved on 0.8% agarose gels. LIN, linear; M1, 1 kb Generuler marker (Fermentas); M2, linearized and untreated target plasmid; OC, open circular; SC, supercoiled plasmid. **a**, TtAgo expression vector pWUR702. **b**, Target plasmid pWUR708, which shares no sequence identity with expression vector pWUR702 or pRARE. Additionally, synthetic (Syn.) ssDNA guides were added to the reactions with pWUR708 (lane 5–8).

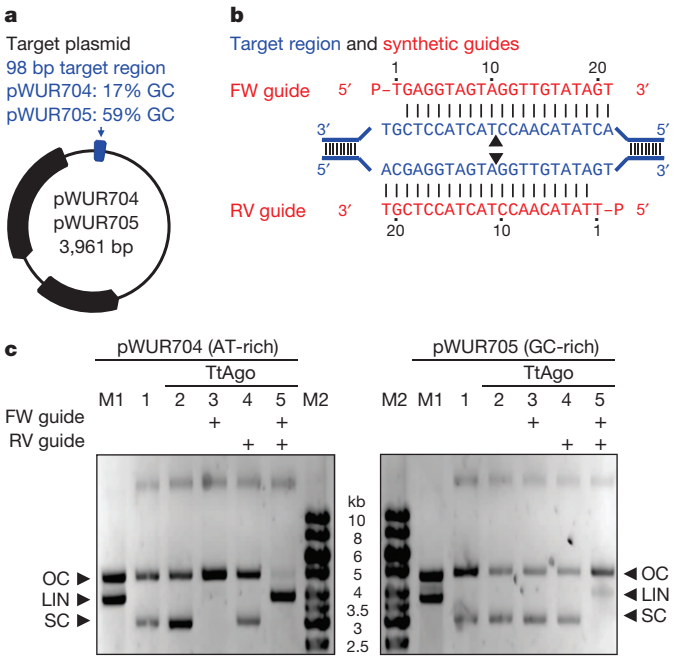

Figure 4 | TtAgo cleaves plasmids by nicking two strands. **a**, Plasmids pWUR704 and pWUR705 contain a 98 bp target region with a GC content of 17% or 59%, respectively, as indicated in blue (for details, see Extended Data Fig. 5a, b). **b**, Part of the pWUR704 and pWUR705 target site (indicated in blue) and complementary ssDNA guides used in this experiment (indicated in red). Black triangles indicate predicted cleavage sites. **c**, 0.8% agarose gels loaded with pWUR704 and pWUR705 plasmids that were incubated without proteins (lane 1), or with TtAgo (lane 2), TtAgo–forward (FW) guide complex (lane 3), TtAgo–reverse (RV) guide complex (lane 4), or TtAgo–FW and TtAgo–RV guide complexes. LIN, linear; M1, open circular and linear pWUR704 or pWUR705; M2, 1 kb Generuler marker (Fermentas); OC, open circular; SC, supercoiled plasmid.

propose to refer to these guides of TtAgo as small interfering DNAs (siDNAs).

To gain insight into the molecular mechanism of dsDNA cleavage by TtAgo, we performed additional *in vitro* plasmid cleavage assays using purified TtAgo loaded with synthetic siDNAs. Negatively supercoiled plasmids (isolated from *E. coli*) were used, because at least 95% of all plasmids isolated from *T. thermophilus* have a negatively supercoiled topology[16,17]. Negative supercoiling facilitates melting of the DNA duplex, especially at elevated temperatures[18–20]. Target plasmids pWUR704 and pWUR705 are identical except for the flanking regions of the target site (AT-rich or GC-rich; Fig. 4a). Both plasmids share no sequence similarity with TtAgo expression plasmid pWUR702, and they are not cleaved by TtAgo unless complementary siDNAs are added (Fig. 4c). When supplied with a single 21-nucleotide siDNA, TtAgo nicks the negatively supercoiled plasmid (Fig. 4c, lanes 3, 4), and when supplied with a mixture of two 21-nucleotide siDNAs that target both DNA strands at the same locus, TtAgo linearizes the plasmid (Fig. 4b, c, lane 5). Both nicking and dsDNA cleavage are more efficient when the target sequence is flanked by AT-rich regions (Fig. 4a, c and Extended Data Fig. 5a, b). Interestingly, the same TtAgo–siDNA complexes are not able to cleave linearized plasmids (Extended Data Fig. 5c, d). This suggests that cleavage of dsDNA by TtAgo depends on the negatively supercoiled topology of the target DNA.

Subsequent analysis revealed that the TtAgo–siDNA complex is able to linearize a relaxed, nicked plasmid if its target site is directly opposite the first nick (Extended Data Fig. 5e). If the nicked site is located further away (33 bp) from the target site, linearization of the nicked plasmid occurs only if the target region is AT-rich (Extended Data Fig. 5f, g). Thus, although the negatively supercoiled topology of the plasmid is lost after the primary nick, the nick facilitates local melting of the dsDNA (especially in AT-rich DNA), which allows TtAgo–siDNA complexes to nick the second strand, resulting in a dsDNA break. Like eukaryotic Ago proteins[21], the TtAgo–siDNA complex cleaves a phosphate ester bond between the target nucleotides that base pair with guide nucleotides 10 and 11 (ref. 22). Sequence analysis of a cleaved dsDNA target (Extended Data Fig. 5h) demonstrated that dsDNA breaks also result from nicking both strands at the canonical Ago cleavage site.

While this manuscript was under revision, a characterization of a prokaryotic Ago protein from *Rhodobacter sphaeroides* (RsAgo) was published[23]. Despite similarities in the overall domain architecture of TtAgo and RsAgo, there are major functional differences between these proteins. RsAgo acquires mRNA-derived RNA guides with a 5′ uridine (U), whereas TtAgo acquires DNA guides with a 5′ dC. In both proteins, guides complementary to plasmids are over-represented. However, RsAgo lacks a functional catalytic site and functions by target-binding alone. TtAgo, on the other hand, harbours a functional catalytic site allowing cleavage of both single- and double-stranded targets.

On the basis of our findings, we propose a model for DNA interference by TtAgo. On the entry of plasmid DNA into the cell, TtAgo acquires siDNA guides (13–25 nucleotides in length) from the invader. Although the mechanism of guide acquisition by TtAgo is unknown, the requirement of an intact catalytic site suggests involvement of the nuclease itself. TtAgo is loaded with siDNAs that are preferentially derived from plasmids; as such, single guides may allow for neutralization of multi-copy invaders. Combining our *in vivo* and *in vitro* data, we speculate that TtAgo uses siDNA guides to specifically cleave ssDNA targets, such as DNA taken up by the natural competence system[5] or replication intermediates. The siDNA–TtAgo complex also targets negatively supercoiled dsDNA, which results in plasmid nicking. Especially in the case of plasmid DNA, single-strand breaks will result in loss of the supercoiled topology and, as such, in decreased transcription levels[24]. Furthermore, if the nick site is located in an AT-rich region, TtAgo loaded with an siDNA that targets the opposite strand may generate

a dsDNA break, potentially leading to degradation of the plasmid by other nucleases. The observation that invading DNA elements generally have a lower GC content than their hosts[25] may explain self/non-self discrimination by TtAgo. Whereas the eukaryotic Ago protein is a key component of sophisticated multi-enzyme systems for RNA-guided RNA interference, we reveal the biochemical activity and functional importance of an evolutionarily related enzyme in prokaryotes that protects its host against mobile genetic elements through DNA-guided DNA interference.

METHODS SUMMARY

T. thermophilus HB27, HB27^{EC}, and two derivatives of the HB27 strain, HB27Δ*ago* and HB27Δ*ago*::^{s}*ago*, were used for plasmid transformation experiments. Plasmid pMHPnqosGFP was isolated from HB27 and HB27Δ*ago*. RNA for RNA-seq analysis was purified from HB27 and HB27Δ*ago* during mid-log-phase growth. Strep(II)-tagged TtAgo was heterologously produced from a plasmid in *E. coli* KRX (Promega) and purified by affinity purification before analyses of co-purified nucleic acids. Guides co-purified with TtAgo or synthetic guides were used in *in vitro* TtAgo cleavage assays using synthetic ssDNA or dsDNA plasmid as targets.

Online Content Any additional Methods, Extended Data display items and Source Data are available in the online version of the paper; references unique to these sections appear only in the online paper.

Received 30 July; accepted 19 December 2013.

Published online 16 February 2014.

1. Ketting, R. F. microRNA biogenesis and function: an overview. *Adv. Exp. Med. Biol.* **700,** 1–14 (2011).
2. Joshua-Tor, L. & Hannon, G. J. Ancestral roles of small RNAs: an Ago-centric perspective. *Cold Spring Harb. Perspect. Biol.* **3,** a003772 (2011).
3. Makarova, K. S., Wolf, Y. I., van der Oost, J. & Koonin, E. V. Prokaryotic homologs of Argonaute proteins are predicted to function as key components of a novel system of defense against mobile genetic elements. *Biol. Direct* **4,** 29 (2009).
4. Koyama, Y., Hoshino, T., Tomizuka, N. & Furukawa, K. Genetic transformation of the extreme thermophile *Thermus thermophilus* and of other *Thermus* spp. *J. Bacteriol.* **166,** 338–340 (1986).
5. Averhoff, B. Shuffling genes around in hot environments: the unique DNA transporter of *Thermus thermophilus*. *FEMS Microbiol. Rev.* **33,** 611–626 (2009).
6. Gregory, S. T. & Dahlberg, A. E. Transposition of an insertion sequence, IS*Tth7*, in the genome of the extreme thermophile *Thermus thermophilus* HB8. *FEMS Microbiol. Lett.* **289,** 187–192 (2008).
7. Liu, J. *et al.* Argonaute2 is the catalytic engine of mammalian RNAi. *Science* **305,** 1437–1441 (2004).
8. Wang, Y., Sheng, G., Juranek, S., Tuschl, T. & Patel, D. J. Structure of the guide-strand-containing argonaute silencing complex. *Nature* **456,** 209–213 (2008).
9. Yuan, Y. R. *et al.* Crystal structure of *A. aeolicus* argonaute, a site-specific DNA-guided endoribonuclease, provides insights into RISC-mediated mRNA cleavage. *Mol. Cell* **19,** 405–419 (2005).
10. Ma, J. B. *et al.* Structural basis for 5′-end-specific recognition of guide RNA by the *A. fulgidus* Piwi protein. *Nature* **434,** 666–670 (2005).
11. Nakanishi, K., Weinberg, D. E., Bartel, D. P. & Patel, D. J. Structure of yeast Argonaute with guide RNA. *Nature* **486,** 368–374 (2012).
12. Wang, Y. *et al.* Structure of an argonaute silencing complex with a seed-containing guide DNA and target RNA duplex. *Nature* **456,** 921–926 (2008).
13. Wang, Y. *et al.* Nucleation, propagation and cleavage of target RNAs in Ago silencing complexes. *Nature* **461,** 754–761 (2009).
14. Frank, F., Sonenberg, N. & Nagar, B. Structural basis for 5′-nucleotide base-specific recognition of guide RNA by human AGO2. *Nature* **465,** 818–822 (2010).
15. Frank, F., Hauver, J., Sonenberg, N. & Nagar, B. *Arabidopsis* Argonaute MID domains use their nucleotide specificity loop to sort small RNAs. *EMBO J.* **31,** 3588–3595 (2012).
16. Collin, R. G., Morgan, H. W., Musgrave, D. R. & Daniel, R. M. Distribution of reverse gyrase in representative species of eubacteria and archaebacteria. *FEMS Microbiol. Lett.* **55,** 235–240 (1988).
17. Charbonnier, F. & Forterre, P. Comparison of plasmid DNA topology among mesophilic and thermophilic eubacteria and archaebacteria. *J. Bacteriol.* **176,** 1251–1259 (1994).
18. Duguet, M. The helical repeat of DNA at high temperature. *Nucleic Acids Res.* **21,** 463–468 (1993).
19. Westra, E. R. *et al.* CRISPR immunity relies on the consecutive binding and degradation of negatively supercoiled invader DNA by Cascade and Cas3. *Mol. Cell* **46,** 595–605 (2012).
20. Bates, A. D. & Maxwell, A. *DNA Topology* 2nd edn (Oxford Univ. Press, 2005).
21. Elbashir, S. M., Martinez, J., Patkaniowska, A., Lendeckel, W. & Tuschl, T. Functional anatomy of siRNAs for mediating efficient RNAi in *Drosophila melanogaster* embryo lysate. *EMBO J.* **20,** 6877–6888 (2001).
22. Sheng, G. *et al.* Structure-based cleavage mechanism of *Thermus thermophilus* Argonaute DNA guide strand-mediated DNA target cleavage. *Proc. Natl Acad. Sci. USA* **111,** 652–657 (2013).
23. Olovnikov, I., Chan, K., Sachidanandam, R., Newman, D. K. & Aravin, A. A. Bacterial Argonaute samples the transcriptome to identify foreign DNA. *Mol. Cell* **51,** 594–605 (2013).
24. Travers, A. & Muskhelishvili, G. DNA supercoiling—a global transcriptional regulator for enterobacterial growth? *Nature Rev. Microbiol.* **3,** 157–169 (2005).
25. Rocha, E. P. C. & Danchin, A. Base composition bias might result from competition for metabolic resources. *Trends Genet.* **18,** 291–294 (2002).

Supplementary Information is available in the online version of the paper.

Acknowledgements We want to thank A. Hidalgo, C. E. César, M. Davids and R. H. J. Staals for advice on experimental procedures. Furthermore, we would like to thank R. Engelhart, B. van Genugten, G. Göertz and R. Stolk for experimental contributions. This work was financially supported by grants from the Netherlands Organization of Scientific Research (NWO) to J.O. (NWO-TOP, 854.10.003), and to S.J.J.B. (NWO Vidi , 864.11.005), and by project BIO2010-18875 from the Spanish Ministry of Science and Innovation, and an Institutional Grant from the Fundación Ramón Areces to CBMSO (J.B.).

Author Contributions M.M.J. and J.H.J. made genomic *T. thermophilus* mutants under the supervision of J.v.d.O. *T. thermophilus* experiments were performed by D.C.S., M.M.J. and J.H.J. under the supervision of J.B., S.J.J.B. and J.v.d.O. D.C.S. and E.R.W. purified RNA for RNA-seq, and D.C.S. analysed RNA-seq data under the supervision of S.J.J.B. and J.v.d.O. D.C.S. and A.P.S. performed experiments in which TtAgo expression in *T. thermophilus* was shown using mass spectrometry. D.C.S., M.M.J. and J.H.J. made all plasmid constructs under the supervision of S.J.J.B., J.B. and J.v.d.O. D.C.S., E.R.W. and Y.Z. purified and analysed TtAgo guides. *In vitro* activity assays were designed and analysed by D.C.S., S.J.J.B., Y.W., D.J.P. and J.v.d.O., and performed by D.C.S. and Y.Z. under the supervision of S.J.J.B. and J.v.d.O. All authors read and approved the submitted manuscript.

Author Information The RNA-seq data discussed in this publication have been deposited in NCBI's Gene Expression Omnibus under accession number GSE52738. The siDNA sequence data discussed in this publication have been deposited in NCBI s BioSample database and are accessible under accession number SAMN02593821. Reprints and permissions information is available at www.nature.com/reprints. The authors declare no competing financial interests. Readers are welcome to comment on the online version of the paper. Correspondence and requests for materials should be addressed to J.v.d.O. (john.vanderoost@wur.nl).

METHODS

Strains. For *in vivo* experiments, *T. thermophilus* HB27 (ATCC BAA-163, DSM 7039 and NBRC 101085) was used, which is referred to in this manuscript as HB27 or wild type. Furthermore, HB27^{EC}, and two genomic variants of the HB27 strain, HB27Δ*ago* (knockout strain) and HB27Δ*ago::*^{s}*ago* (knockout strain complemented with *strep(II)-tag-ago* fusion and kanamycin resistance marker insert), were used (Fig. 1 and Extended Data Table 4a).

Genomic mutants. HB27 genomic DNA including megaplasmid pTT27 was purified using the FastDNA SPIN Kit for Soil (MP Biomedicals). The genomic regions directly upstream (1 kb) and downstream (2.4 kb) of the *ago* gene (TT_P0026) were PCR amplified from *T. thermophilus* HB27 genomic DNA. These genomic regions contained pTT27 base-pair positions 26047–25061 (upstream sequence) and 22996–20583 (downstream sequence). The amplified DNA was cloned into the pUC18 vector (Extended Data Table 5), and the insert was transferred to pK18 (ref. 26) to generate pWUR701 (Extended Data Table 5). Strain HB27 was grown to an $OD_{600\,nm}$ of 0.4 in TTH medium (0.8% (w/v) bacto-tryptone, 0.4% (w/v) yeast extract, 51.3 mM NaCl, pH to 7.5 with NaOH, dissolved in mineral water (Evian)). 0.5 ml of the culture was transferred to a new tube and naturally transformed by the addition of 1 μg plasmid pWUR701. The culture was incubated overnight in a shaker incubator at 65 °C and plated on TTH plates with 30 μg ml^{-1} kanamycin. Cells were repetitively streaked on non-selective TTH plates and grown in non-selective TTH medium until kanamycin^{R} was lost. Genomic DNA of kanamycin^{S} cells was purified using the FastDNA SPIN Kit for Soil (MP Biomedicals) and loss of the *ago* gene was confirmed by PCR amplification of genomic DNA and sequencing of the target region. This strain is named HB27Δ*ago*, or knockout strain.

The genes encoding Strep(II)-tagged TtAgo protein and kanamycin^{R} marker with upstream pSLPa promoter were PCR amplified from pWUR627 and pMK184 (ref. 28), respectively (Extended Data Table 5). PCR products were cloned into pWUR676 as indicated in Extended Data Table 5. HindIII-linearized pWUR676 was used to transform strain HB27Δ*ago* as described earlier. This strain is named HB27Δ*ago::*^{s}*ago* (Fig. 1). Genomic DNA was purified using the FastDNA SPIN Kit for Soil (MP biomedicals) and insertion of the ^{s}*ago*-kanamycin^{R} cassette was confirmed by PCR amplification from genomic DNA and sequencing of the target region.

Transformations. *T. thermophilus* strains were cultivated in TTH medium in a 65 °C shaker incubator until an $OD_{600\,nm}$ of 0.4 was reached. The culture was diluted 1:1 in pre-warmed TTH medium and incubated for another hour at 65 °C. 0.5 ml of the culture was transferred to a new tube, which was incubated at 65 °C for 30 min. One-hundred nanograms of plasmid pMK184 or pMHPnqosGFP was added and the mixture was incubated for 4 h at 65 °C without shaking, after which it was serial diluted and plated on TTH plates (TTH medium solidified with 1.5% agar) and on selective TTH plates (TTH plates supplied with 50 μg ml^{-1} kanamycin or 100 μg ml^{-1} hygromycin). After 48 h of incubation at 65 °C, colonies were counted. Competence was determined as the amount of kanamycin^{R} or hygromycin^{R} colony-forming units (c.f.u.; counted on selective plates) per μg DNA, divided by total c.f.u. (counted on non-selective plates). To show relative competence, HB27 wild-type transformation efficiency was set to 1, with the competences of other strains normalized against this number.

DNA purification. For plasmid purification, *T. thermophilus* HB27 and HB27Δ*ago* cultures were cultivated in triplicates in TTH medium supplied with 30 ng μl^{-1} kanamycin and 100 ng μl^{-1} hygromycin. Five $OD_{600\,nm}$ units of each overnight culture were harvested and plasmids were isolated with the Fermentas GeneJET plasmid Miniprep Kit (Thermo Scientific) according to the manual provided by the manufacturer and quantified using a NanoDrop ND1000 spectrophotometer. For complete DNA (containing both genomic and plasmid DNA) purification, *T. thermophilus* HB27 and HB27Δ*ago* cultures were cultivated in triplicates to an $OD_{600\,nm}$ of 0.500. One $OD_{600\,nm}$ unit was harvested and complete DNA was isolated using the JGI 'bacterial genomic DNA isolation using CTAB' protocol. 2.5 μg DNA of each purification was resolved on 0.8% agarose gels and stained with SYBR Safe Nucleic Acid Stain (Invitrogen), visualized using a G:BOX Chemi imager and analysed using GeneTools analysis software (Syngene).

RNA sequencing. Triplicate *T. thermophilus* strains were cultivated in 20 ml TTH medium in a 65 °C shaker incubator overnight. Cultures were diluted 1/100 and grown to an $OD_{600\,nm}$ of 0.5, after which cells were harvested by centrifugation. After harvesting, RNA was purified using the mirVana RNA isolation kit (Ambion) according to the instructions provided by the manufacturer. Biological triplicates of purified RNA were sequenced by BaseClear BV by Illumina sequencing. Reads were mapped on genomes and plasmid using Rockhopper[29], but rather than using the programs calculated expression rates and significance, the percentage of raw counts mapped on each gene were normalized against the total number of raw counts mapped on the genome. Variance in expression was calculated by dividing the average of the triplicate normalized counts mapped on single genes in strain HB27 by the average of the triplicate normalized counts mapped on the same gene in strain HB27Δ*ago*.

TtAgo expression and purification from *E. coli* KRX. The *ago* gene was PCR amplified from *T. thermophilus* (ATCC 27634) genomic DNA (gene TTHB0068, base positions on pTT27: 61573–59516), and directionally cloned into a pET-52b(+) expression vector as indicated in Extended Data Table 5 (pWUR627). By introduction of mutations according to the QuikChange Site-Directed Mutagenesis Kit instruction manual (Stratagene), pWUR642 was generated (Extended Data Table 5). The inserts of pWUR627 and pWUR642 were PCR amplified and ligated into pCDF-1b as indicated in Extended Data Table 5 (pWUR702 and pWUR703). These plasmids were transformed into *E. coli* KRX (Promega) simultaneously with pRARE (Novagen), purified from *E. coli* Rosetta DE3 (Novagen). Strains were cultivated in LB medium containing the corresponding antibiotics (50 ng ml^{-1} streptomycin, 34 μg ml^{-1} chloramphenicol) in a shaker incubator at 37 °C. When the culture reached an $OD_{600\,nm}$ of 0.7–0.8, cells were cold-shocked by incubation in an ice bath for 15 min. Expression was induced by adding isopropyl-β-D-thiogalactoside (IPTG) and L-Rhamnose to a final concentration of 1 mM and 0.1% (w/v), respectively, and expression was continued for 16 h in a shaker incubator at 20 °C. Cells were harvested by centrifugation. For plasmid quantification, plasmids were isolated from 5 $OD_{600\,nm}$ units of harvested cells using the Fermentas GeneJET plasmid Miniprep Kit (Thermo Scientific) according to the manual provided by the manufacturer and quantified using a NanoDrop ND1000 spectrophotometer. For TtAgo purification, harvested cells were resuspended in Buffer I (20 mM Tris-HCl pH 8, 1 M NaCl, supplied with either 2 mM $MnCl_2$ or 2 mM $MgCl_2$), and disrupted using a French pressure cell. Expressed proteins have an N-terminal Strep(II)-tag and were isolated using Strep-Tactin affinity chromatography (IBA) with an adapted protocol. Before loading of the cell-free extract, columns were equilibrated in Buffer I. After loading, columns were washed with 9 column volumes of Buffer I and with 9 column volumes of Buffer II (20 mM Tris-HCl pH 8, 0.5 M NaCl, supplied with 2 mM $MnCl_2$). Proteins were eluted in Buffer III (Buffer II supplemented with 2.5 mM *d*-Desthiobiotin (Sigma-Aldrich)). For purification of TtAgo used in Mn/Mg gradient experiments, no Mn or Mg was added to purification buffers. For other activity assays, $MnCl_2$ or $MgCl_2$ was added to all buffers at a final concentration of 0.5 mM.

TtAgo purification from *T. thermophilus*. HB27Δ*ago::*^{s}*ago* was cultivated in TTH medium supplemented with 30 ng ml^{-1} kanamycin at 65 °C. After overnight growth, cells were harvested and TtAgo was purified as described earlier. After purification, elution fractions were resolved on SDS–PAGE gels and purified proteins were stained using Coomassie brilliant blue stain. A band corresponding to the region with the molecular weight of Argonaute (75–80 kDa) was excised from the gel and subjected to in-gel digestion using a Perkin Elmer Janus Automated Workstation. Peptide mixtures were injected onto a nanoACQUITY UPLC (Waters Corporation) coupled to a LTQ-Orbitap XL (Thermo Fisher Scientific) via an Advion Biosciences Nanomate. Peptides were eluted over a 30 min gradient (5–40% ACN). MaxQuant (v.1.4.1.2) and its embedded Andromeda search engine were used to search the data against a database containing *T. thermophilus* sequences extracted from Uniprot (8 August 2013). Methionine oxidation was used as a variable modification and a maximum of two missed trypsin cleavages were allowed. Peptide and protein posterior error probabilities (PEP) were calculated using a target-decoy search using the revert scheme. The light version of intensity-based absolute quantification (iBAQ) was used to rank the identified proteins by estimated relative abundance.

Guide co-purification and sequencing. Proteinase K (Ambion) and $CaCl_2$ (final concentration, 5 mM) were added to purified proteins and samples were incubated for 1 h at 37 °C. Nucleic acids were separated from protein content using Roti phenol/chloroform/isoamyl alcohol pH 7.5–8.0 (Carl Roth GmbH) and further purified by ethanol precipitation. Precipitation was performed overnight at −20 °C in the presence of linear polymerized acrylamide as carrier.

Purified nucleic acids were [γ-^{32}P]ATP labelled with T4 PNK (Fermentas) in exchange- or forward-labelling reactions and thereafter separated from free [γ-^{32}P]ATP using a Sephadex G-25 column (GE). Labelled nucleic acids were incubated with nucleases (DNase-free RNase A (Fermentas), RQ1 RNase-free DNaseI (Promega) or P1 nuclease (Sigma)) for 1 h at 37 °C. After nuclease treatment, samples were mixed with Loading Buffer (95% (deionized) formamide, 5 mM EDTA, 0.025% SDS, 0.025% bromophenol blue and 0.025% xylene cyanol), heated for 5 min at 95 °C and resolved on 15% or 20% denaturing polyacrylamide gels. Radioactivity was captured from gels using phosphor screens.

Nucleic acids were purified from TtAgo and treated with RNaseA, as described earlier. The small 5′-phosphorylated DNA molecules were poly-adenylated at their 3′ end using recombinant terminal deoxynucleotidyl transferase (TdT, Invitrogen), according to the instructions of the manufacturer. After purification of the product using the QIAquick nucleotide removal kit (Qiagen), 5′-phosphorylated and 3′-polyadenylated products were ligated to the 3′ end of oligonucleotide BG4409

(Extended Data Table 4b) using T4 RNA ligase (Ambion), according to the instructions of the manufacturer. After purification of the product using the QIAquick nucleotide removal kit (Qiagen), the product was PCR amplified using primers BG4409 and BG4436 (anchored poly-T primer (partially degenerate); Extended Data Table 4b). The PCR amplification product was gel purified using the GeneJET gel extraction kit (Fermentas) and sent for sequencing by Imagif, Plateforme de Séquençage à Haut Débit by Illumina sequencing with an adapted RNA-seq protocol. Sequences were analysed with FastQC software (Babraham Bioinformatics). After mapping on genome and plasmids, duplicate reads were removed using SAMtools software[26], to exclude a bias for preferentially PCR amplified reads in downstream analysis. Unique read data sets were re-analysed with FastQC software and remapped on genome and plasmid DNA using Tablet software (James Hutton Institute)[28].

DNA guides and targets. The sequence of guide BG3466 is based on *let-7* miRNA, and has been used before in experiments performed with TtAgo[8,12,13], whereas the sequence of guide BG4017 is based on the reverse complementary sequence of *let-7* miRNA (Extended Data Table 4b). Both guides have a 5′ phosphate, are 21-nucleotides long and have been PAGE purified after synthesis. Oligonucleotides BG4262–BG4265 (Extended Data Table 4b) were used in activity assays as an ssDNA target or mixed together with 2× STE buffer (20 mM Tris-HCl pH 8, 100 mM NaCl, 2 mM EDTA) in a 1:1:2 ratio (BG4262:BG4263:2× STE or BG4264:BG4265:2× STE) and incubated at 95 °C for 5 min. Samples were cooled down to room temperature (20 °C). Annealed oligonucleotides were used as inserts for plasmid pWUR677 (generated from pFU98)[29] to generate pWUR704 and pWUR705. For experiments with nicked and linearized targets, pWUR704 and pWUR705 were treated with Nb.BsmI or SpeI, respectively. Plasmid pWUR708 was generated as pWUR704 and pWUR705 but with annealed BG3467 and BG3468 oligonucleotides as insert.

Activity assays. Purified TtAgo, ssDNA or ssRNA guides, and ssDNA targets (Extended Data Tables 4b, 5) were mixed in 5:1:1 ratio (TtAgo:guide:target) in 2× Reaction Buffer (20 mM Tris-HCl pH 8, 250 mM NaCl supplied with varying concentrations of $MnCl_2$ or $MgCl_2$). Reaction mixtures were incubated for 1 h at 75 °C. Reactions were stopped by the addition of Loading Buffer and heated for 5 min at 95 °C before the samples were resolved on 15% or 20% denaturing polyacrylamide gels. Gels were stained using SYBR gold Nucleic Acid Gel Stain (Invitrogen) and nucleic acids were visualized using a G:BOX Chemi imager (Syngene). Because DNA-guided cleavage of ssDNA is observed in the presence of 5–10 μM Mn^{2+} (Extended Data Fig. 5j), but comparable cleavage levels are observed in the presence of Mg^{2+} only at tenfold higher concentrations (Extended Data Fig. 5j), all activity assays were performed in the presence of 0.5 mM $MnCl_2$.

Purified TtAgo, ssDNA guides and plasmid targets were mixed in a 25:5:1 ratio (TtAgo:guide:target) in 2× Reaction Buffer supplemented with 0.5 mM $MnCl_2$. Samples were incubated for 16 h at 75 °C. Reactions were stopped by adding Proteinase K solution (Ambion) and $CaCl_2$ (final concentration, 5 mM) and samples were incubated for 1 h at 65 °C. Samples were mixed with 6× loading dye (Fermentas) before they were resolved on 0.8% agarose gels. Agarose gels were stained with SYBR safe or SYBR gold Nucleic Acid Gel Stain (Invitrogen) and nucleic acids were visualized using a G:BOX Chemi imager (Syngene).

Plasmid pWUR704 was linearized with TtAgo–siDNA complexes as described earlier. The DNA was purified from the activity assay sample by PCI extraction followed by ethanol precipitation. Purified DNA was cut either by XbaI or by NheI. Restriction site overhangs were filled in with Klenow Fragment (Thermo Scientific) according to the manual provided by the manufacturer. Blunt-end linear plasmid was closed by T4 ligase ligation according to the manual provided by the manufacturer (Thermo Scientific). Ligated plasmids were treated with HindIII (in the case of the XbaI-treated plasmids) or SalI (in the case of NheI-treated plasmids) to eliminate the possible background of the original plasmid. Plasmids were transformed to NEB 5-α *E. coli* competent cells (New England Biolabs) according to the manual provided by the manufacturer. Colonies were picked, grown overnight in LB medium at 37 °C and miniprepped with the Fermentas GeneJET Plasmid Miniprep Kit (Thermo Scientific). Purified plasmids were sent to GATC Biotech (Germany) for target site sequencing.

Statistical analysis. All *P* values stated in this manuscript are calculated by a two-tailed distributed two-sample *t*-test assuming equal variances. For the calculation of *P* values of the transformation efficiencies, competence (calculated as described earlier) from biological duplicates of each strain was used as the input. For the calculation of *P* values of plasmid purification, plasmid DNA yield of biological triplicates of each strain were used as the input. For the calculation of *P* values of plasmid DNA content of complete DNA purification, plasmid DNA content of biological triplicates of each strain were used as the input. For the calculation of *P* values of differences in expression levels of specific genes, normalized raw mapped counts of biological triplicates of each strain were used as the input. All *P* values calculated are considered to be significant, as for all calculations $P < 0.02$).

26. Li, H. *et al.* The Sequence Alignment/Map format and SAMtools. *Bioinformatics* **25,** 2078–2079 (2009).
27. Laptenko, O. *et al.* pH-dependent conformational switch activates the inhibitor of transcription elongation. *EMBO J.* **25,** 2131–2141 (2006).
28. Milne, I. *et al.* Using Tablet for visual exploration of second-generation sequencing data. *Brief. Bioinform.* **14,** 193–202 (2013).
29. Uliczka, F. *et al.* Monitoring of gene expression in bacteria during infections using an adaptable set of bioluminescent, fluorescent and colorigenic fusion vectors. *PLoS ONE* **6,** e20425 (2011).
30. Cava, F. *et al.* Expression and use of superfolder green fluorescent protein at high temperatures *in vivo*: a tool to study extreme thermophile biology. *Environ. Microbiol.* **10,** 605–613 (2008).
31. Cava, F. *et al.* Control of the respiratory metabolism of *Thermus thermophilus* by the nitrate respiration conjugative element NCE. *Mol. Microbiol.* **64,** 630–646 (2007).

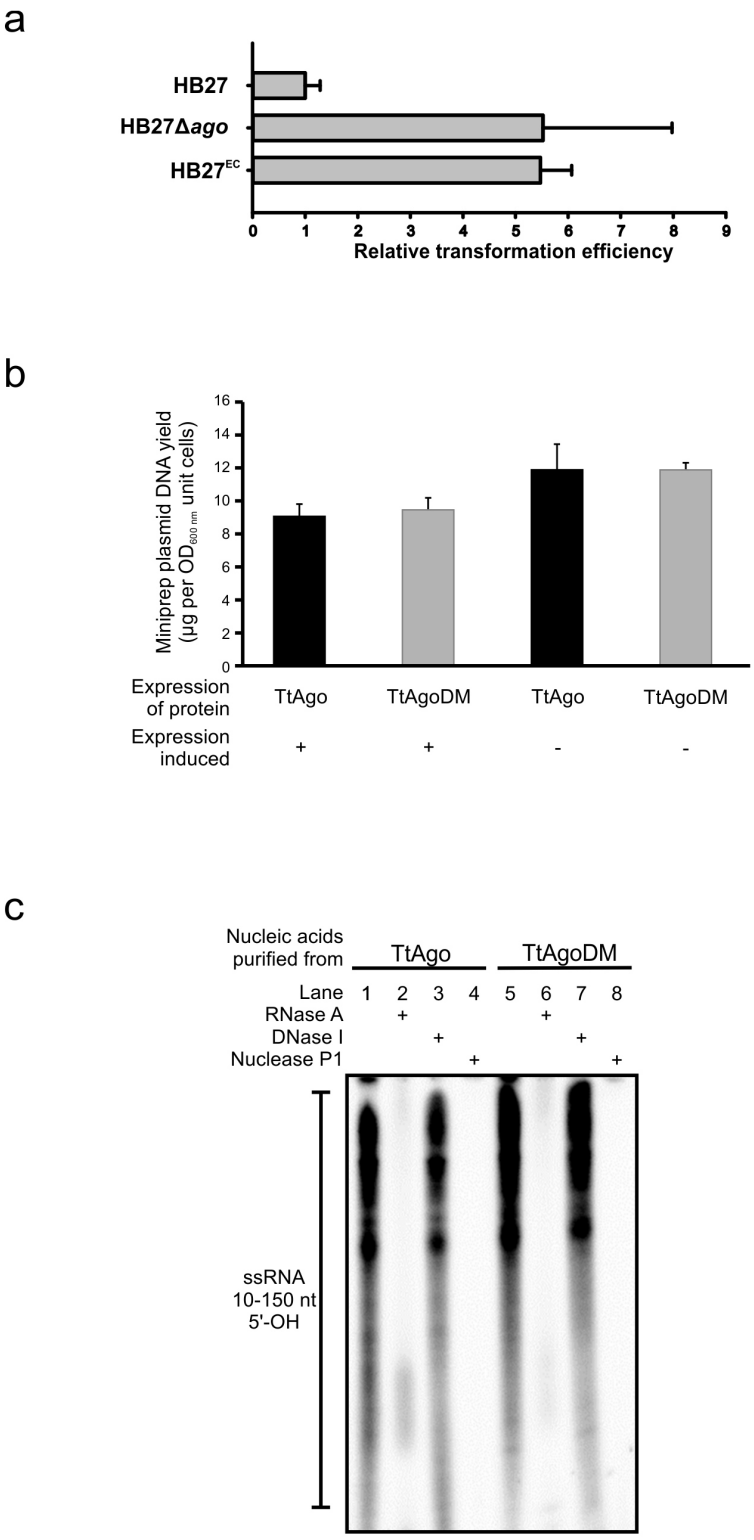

Extended Data Figure 1 | Analyses of TtAgo in *T. thermophilus* and *E.coli*. **a**, TtAgo decreases plasmid transformation efficiency of *T. thermophilus*. Transformation efficiency of different *ago* mutant strains relative to the transformation efficiency of wild-type strain HB27. HB27^{EC} is an HB27 mutant selected for high competence, and HB27Δ*ago* is an *ago* gene knockout strain (Fig. 1a). Strains were transformed with plasmid pMK184 (Extended Data Table 5). Transformations were performed in biological duplicates for each strain. Error bars indicate standard deviations. **b**, Effect on TtAgo expression on plasmid content in *E. coli* KRX. TtAgo and TtAgoDM were expressed in *E. coli* KRX from plasmid pWUR702 and pWUR703. Plasmids were purified from biological triplicate cultures in which expression was induced (+) or not induced (−). Compared with TtAgoDM expression, TtAgo expression in *E. coli* KRX does not lead to reduced plasmid content. Changes in plasmid yield between induced and not induced cultures probably originate from protein expression energy costs. Error bars indicate standard deviations. **c**, 10–150-nucleotide (nt) RNA with 5′-OH group co-purifies with TtAgo. 15% denaturing polyacrylamide gels with nucleic acids co-purified with TtAgo and TtAgoDM. Nucleic acids are phosphorylated in a T4 PNK forward reaction (5′-OH groups, and to a lesser extend 5′-P groups, are labelled) using [γ-^{32}P] ATP, and resolved on 15% denaturing polyacrylamide gels. Nucleic acids were not treated (lane 1, 5), RNaseA treated (lanes 2, 6), DNaseI treated (lane 3, 7) or Nuclease P1 treated (lane 4, 8).

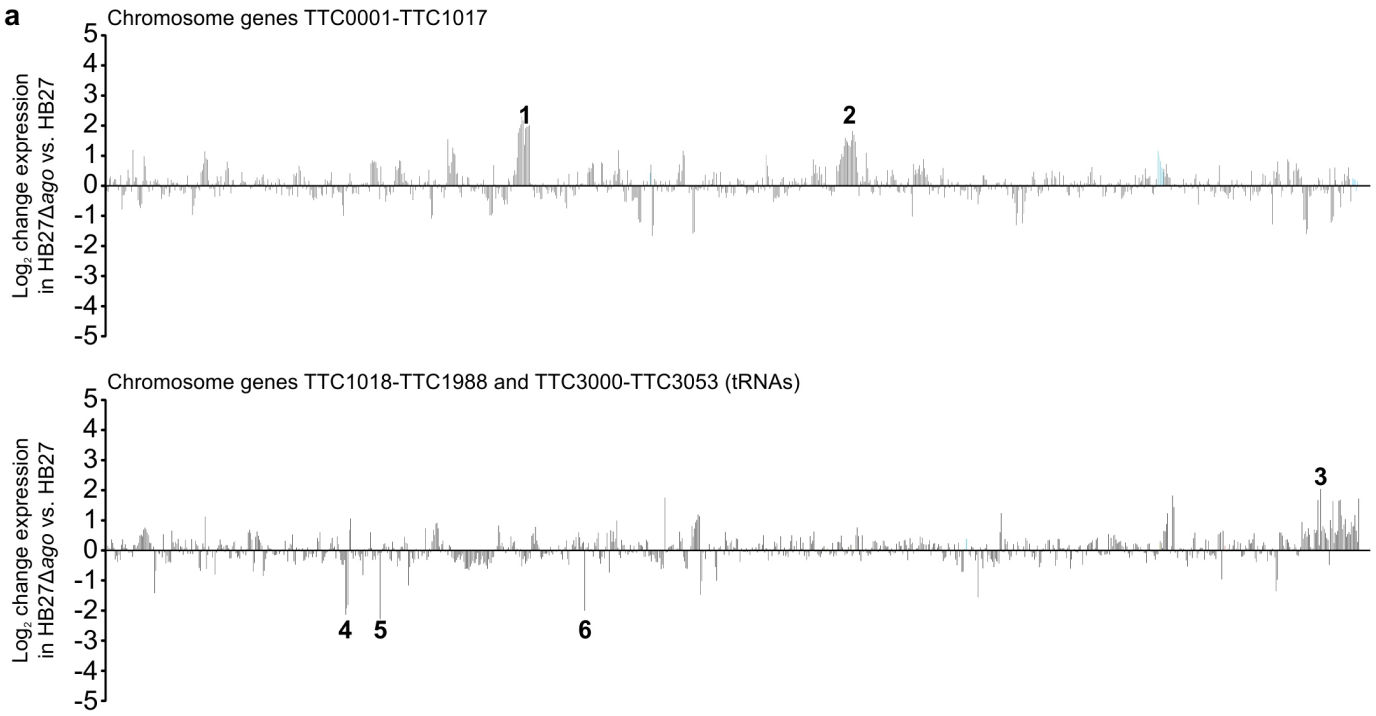

c

	Gene(s)	Encodes	Change in expression (Log_2)	p-value
1	TTC0333-0343	Branched amino acid transport system	1.85	0
2	TTC0597-0603	Branched amino acid transport system	1.43	0.01
3	TTC3000-3053	tRNAs	0.74	0.25
4	TTC1213	1-pyrroline-5-carboxylate dehydrogenase	-2.13	0
5	TTC1241	Acylamino acid releasing enzyme	-2.27	0
6	TTC1407	S-layer protein	-1.99	0
7	TT_P0024	Alkaline phosphatase	-1.64	0
	TT_P0026	TtAgo	< -10.00	0
	TT_P0028	Survival protein SurE	-2.11	0.02
	TT_P0029	Hypothetical conserved protein	-2.63	0.03

Extended Data Figure 2 | Change in transcription of *T. thermophilus* genes after *ago* gene knockout. **a**, **b**, RNA-seq analysis was performed on biological triplicates for each strain. Change in gene expression of genes encoded on the chromosome (**a**) or on the megaplasmid (**b**) is shown as the $\log_2$ of the fold difference in expression of the average of normalized mapped reads on that gene in HB27Δ*ago* compared with the average of normalized mapped reads on that gene in HB27. Peaks corresponding to genes involved in host defence are coloured red, whereas peaks corresponding to genes involved in competence are coloured blue. **c**, Genes or operons containing genes with a $\log_2$ expression change greater than 2 or −2.

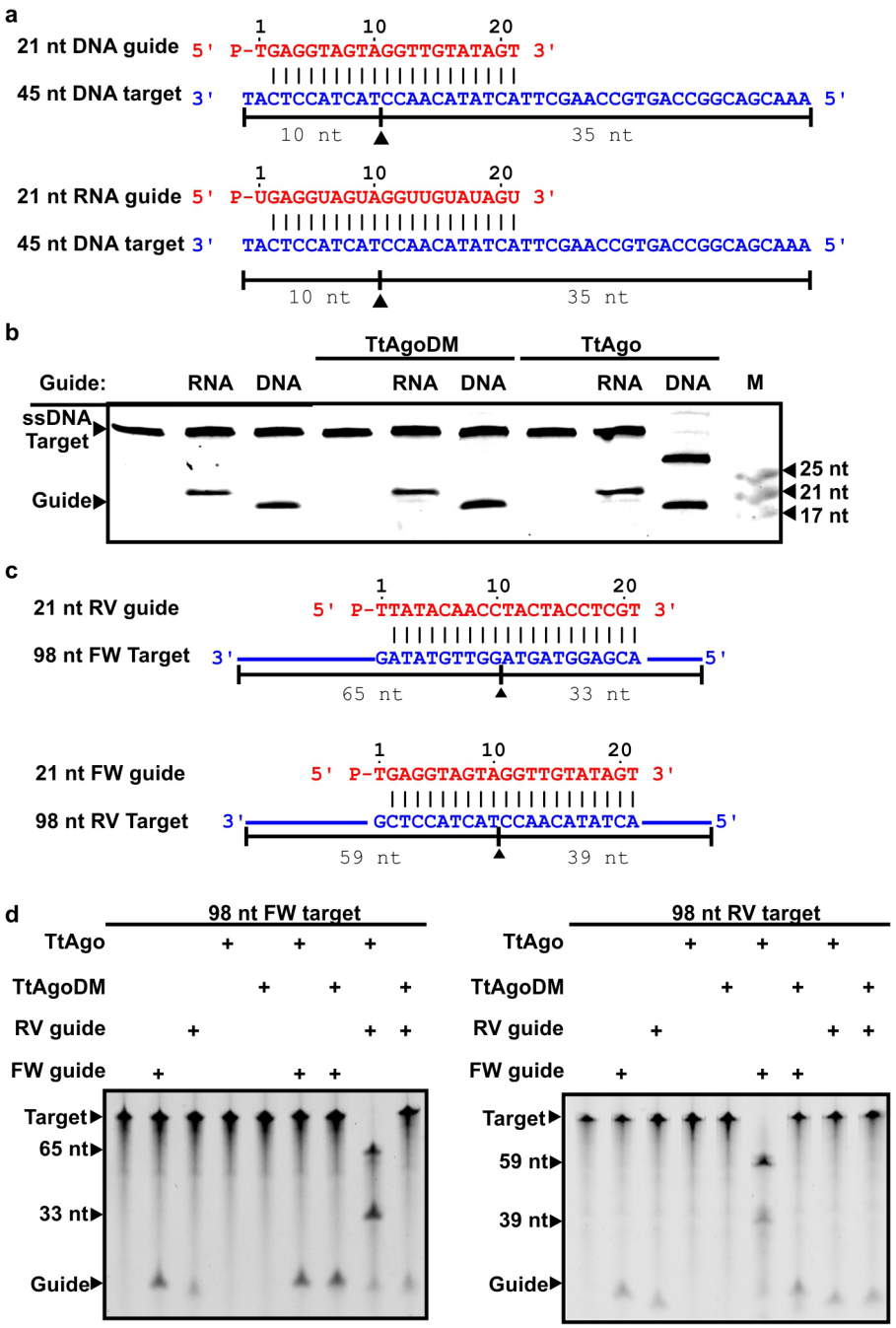

Extended Data Figure 3 | TtAgo cleaves ssDNA using ssDNA guides. **a**, 21-nucleotide (nt) DNA and RNA guides are complementary to the 45-nucleotide DNA targets. Predicted cleavage positions are indicated with a black triangle. **b**, 20% denaturing polyacrylamide gel loaded with samples in which TtAgo and TtAgoDM were provided with an RNA or an DNA guide to cleave a 45-nucleotide ssDNA target. **c**, 21-nucleotide RV and FW DNA guides are complementary to the 98-nucleotide ssDNA targets. Predicted cleavage positions are indicated with a black triangle. **d**, 98-nucleotide ssDNA targets are incubated with TtAgo and TtAgoDM, provided with complementary and non-complementary DNA guides, and resolved on 15% denaturing polyacrylamide gels.

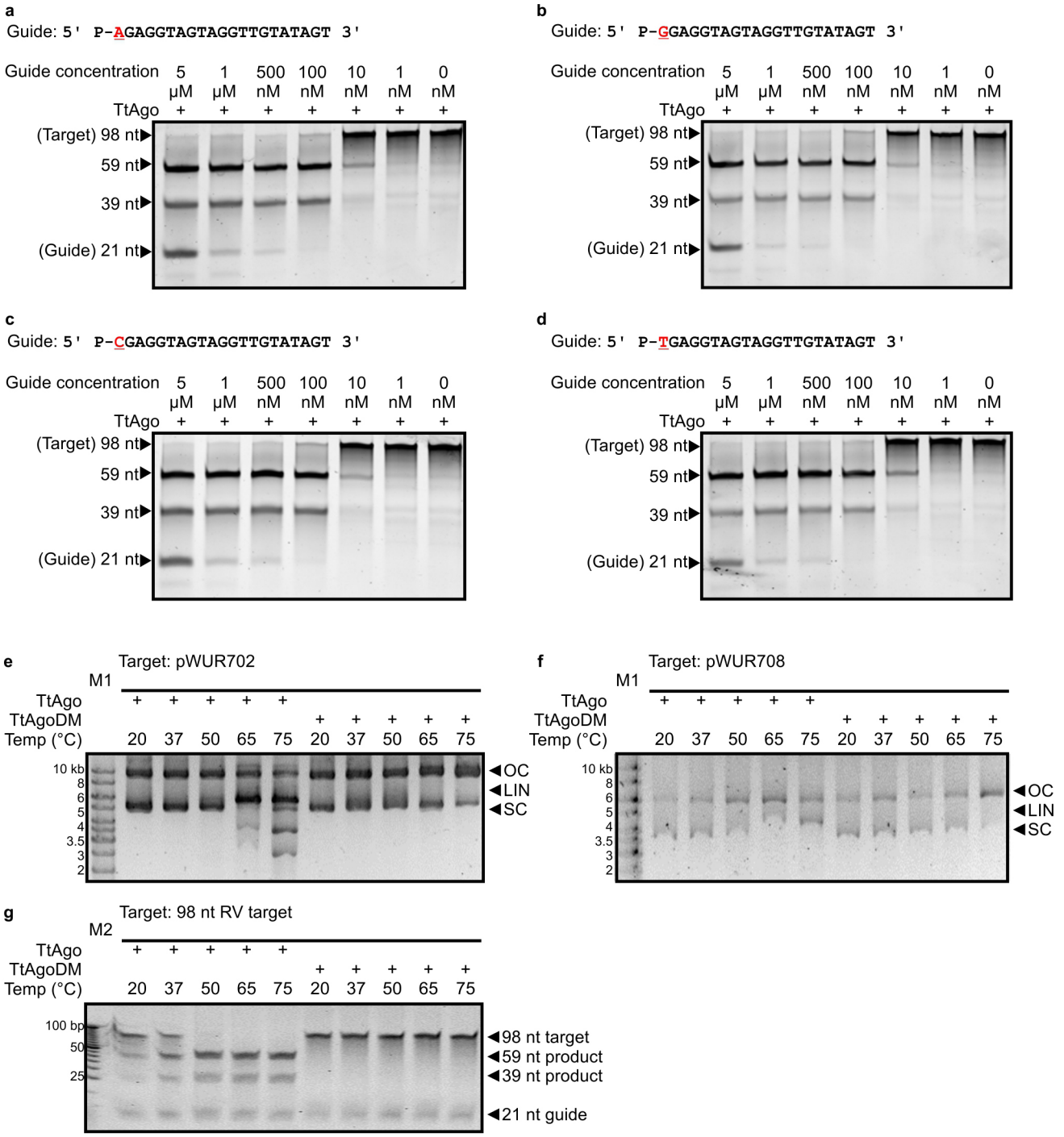

Extended Data Figure 4 | Effect of variation of the 5′-end deoxynucleoside of the siDNA and effect of the temperature on TtAgo cleavage efficiency. **a**–**d**, Cleavage of 98-nucleotide ssDNA target (Extended Data Fig. 3c) by TtAgo loaded with complementary siDNAs containing a different 5′ deoxynucleoside, as shown in red. The concentrations of each siDNA were varied (indicated on top of the gels). Products of the reaction were resolved on 15% denaturing polyacrylamide gels. **e**, TtAgo expression plasmid pWUR702 (no guides added) incubated with TtAgo and TtAgoDM at different temperatures. **f**, pWUR708 plasmid (FW and RV guides added; Fig. 4b) incubated with TtAgo and TtAgoDM at different temperatures, resolved on 0.8% agarose gels. LIN, linear; M1, 1 kb Generuler marker (Fermentas); OC, open circular; SC, supercoiled. **g**, 98-nucleotide RV target cleavage (FW guide added) incubated with TtAgo and TtAgoDM at different temperatures, resolved on a 15% denaturing acrylamide gel. M2, O'RangeRuler 5 bp DNA Ladder (Thermo Scientific).

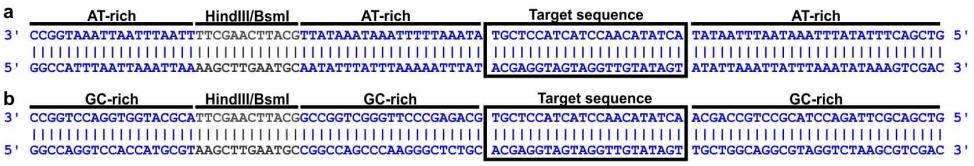

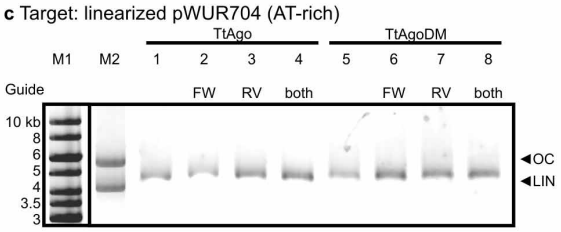

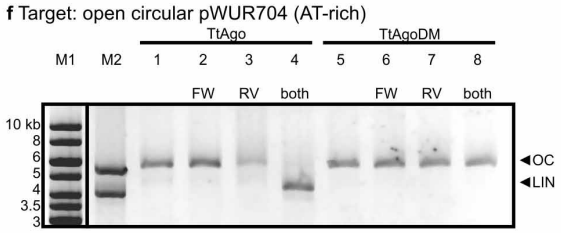

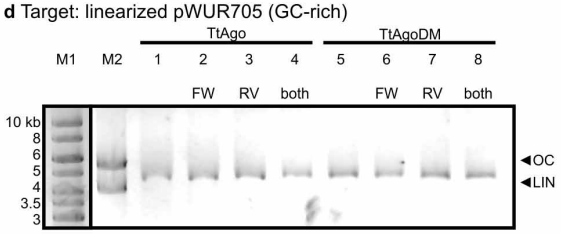

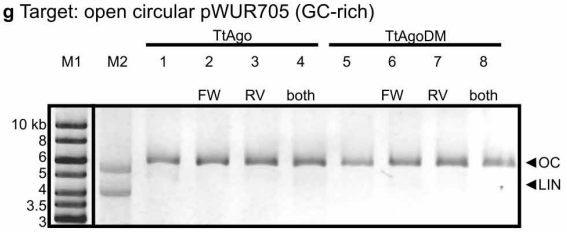

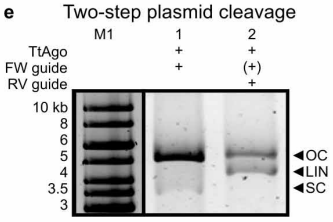

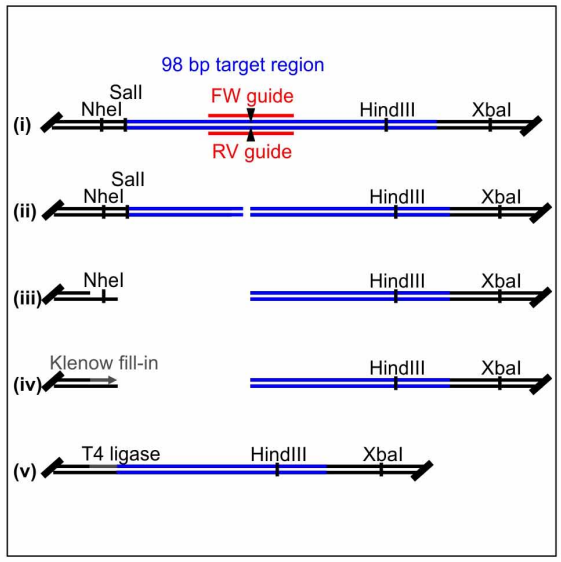

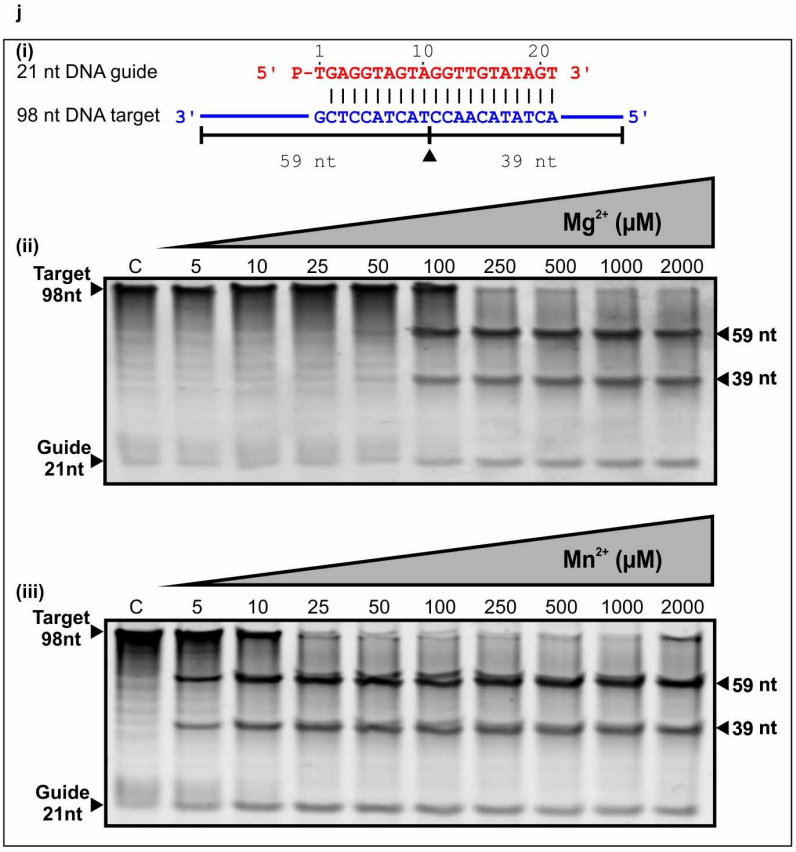

Extended Data Figure 5 | Activity analyses of TtAgo. **a**, **b**, AT-rich (17% GC) insert of pWUR704 (**a**) and GC-rich insert (59% GC) of pWUR705 (**b**). The target sequence is boxed. Restriction sites HindIII and BsmI are indicated in grey. Sequences are displayed in the 3′–5′ direction to allow comparison with Fig. 4b, which shows guide base pairing to this sequence. **c**, **d**, SpeI-linearized plasmid pWUR704 (**c**) and pWUR705 (**d**) incubated with TtAgo–siDNA and TtAgoDM–siDNA complexes targeting both strands of the plasmid, and resolved on 0.8% agarose gels. LIN, linear; M1, 1 kb Generuler marker (Fermentas); M2, open circular and linearized pWUR704 (**c**), or open circular and linearized pWUR705 (**d**); OC, open circular. FW guide: BG3466. RV guide: BG4017. High salt concentration (250 mM NaCl) in the reaction buffer cause the TtAgo-treated samples to run higher in the gel than M1 and M2. **e**, Two-step plasmid cleavage. Target pWUR704 was first nicked by a TtAgo–siDNA complex targeting the first strand (FW guide, lane 1), after which a TtAgo–siDNA complex targeting the other strand was added (RV guide, lane 2). FW guide is still present, and its presence is therefore indicated as (+). LIN, linear; M1, 1 kb Generuler marker (Fermentas); OC, open circular; SC, supercoiled. **f**, **g**, Nb.BsmI-nicked plasmid pWUR704 (**f**) and pWUR705 (**g**) incubated with TtAgo–siDNA and TtAgoDM–siDNA complexes targeting the un-nicked strands of the plasmid (33 bp away from the nicking site), and resolved on 0.8% agarose gels. LIN, linear; M1, 1 kb Generuler marker (Fermentas); M2, open circular and linearized pWUR704 (**a**), or open circular and linearized pWUR705 (**b**); OC, open circular. High salt concentrations (250 mM NaCl) in the reaction buffer cause the TtAgo-treated samples to run higher in the gel than M1 and M2. **h**, TtAgo dsDNA cleavage site analysis. (i) Plasmid pWUR704 with TtAgo–siDNA target sequences. Predicted cleavage sites are indicated with black triangles. (ii) pWUR704 was linearized using TtAgo–siDNA complexes targeting the plasmid on both strands. (iii) The linearized plasmid was cleaved using either NheI (as shown) or XbaI (not shown). (iv) Restriction site overhangs and possible overhangs resulting from TtAgo–siDNA cleavage were filled using Klenow fragment polymerase (Fermentas). (v) Blunt-end DNA was ligated using T4 DNA ligase (Fermentas), after which the plasmid could be transformed and later sequenced to determine the cleavage site. Sequences revealed that TtAgo–siDNA complexes indeed cleaved the target at the predicted locations (as shown in **a**), and are shown in more detail in Fig. 4b and Extended Data Fig. 5a, b. Note that in this picture target sequences are displayed in reversed order compared with Fig. 4b and Extended Data Fig. 5a, b. **j**, TtAgo prefers Mn^{2+} over Mg^{2+} as a divalent cation for cleavage. (i) 21-nucleotide DNA guide and 98-nucleotide ssDNA target used. The predicted cleavage site is indicated with a black triangle. (ii) 98-nucleotide ssDNA target cleavage reaction with TtAgo loaded with a 21-nucleotide siDNA in the presence of increasing concentrations of Mg^{2+}, as indicated on top of the gel. (iii) 98-nucleotide ssDNA target cleavage reaction with TtAgo loaded with a 21-nucleotide siDNA in the presence of increasing concentrations of Mn^{2+}, as indicated. Samples were resolved on 15% denaturing polyacrylamide gels.

Extended Data Table 1 | Expression profile of *T. thermophilus* genes involved in competence and host-defence

a

Genes involved in competence		
Gene	**Encoded protein**	**Log_2 fold change (*P*-value)**
TTC1603	ComEC	0.09 (0.49)
TTC1602	ComEA	-0.05 (0.74)
TTC1873	DprA	0.22 (0.19)
TTC0854	PilA1	1.15 (0.02)
TTC0855	PilA2	0.97 (<0.01)
TTC0856	PilA3	0.82 (<0.01)
TTC0858	PilA4	0.45 (0.17)
TTC1716	PilD	0.40 (0.11)
TTC1622	PilF	0.10(0.11)
TTC0440	PilC	0.43 (<0.01)
TTC1017	PilQ	0.15 (0.30)
TTC0857	ComZ	0.61 (0.05)
TTC1013	PilM	0.25 (0.06)
TTC1014	PilN	0.21 (0.05)
TTC1015	PilO	0.20 (0.43)
TTC1016	PilW	-0.17 (0.12)
TT_P0190	PilA	-0.01 (0.93)

b

Genes involved in host-defence		
Gene	**Encoded protein**	**Log_2 fold change (*P*-value)**
TT_P0026	TtAgo	<-10 (<0.01)
TTC1926	Cas2	0.16 (0.03)
TTC1927	Cas6	0.02 (0.88)
TT_P0101	Cas2	0.18 (0.61)
TT_P0102	Csm1	0.39 (0.04)
TT_P0103	Csm2	0.46 (<0.01)
TT_P0104	Csm3	0.54 (<0.01)
TT_P0105	Csm4	0.64 (0.01)
TT_P0106	Csm5	0.52 (<0.01)
TT_P0107	Csx1	0.28 (0.07)
TT_P0115	Cmr2	0.32 (0.06)
TT_P0116	Cmr3	0.30 (0.16)
TT_P0117	Cmr1	0.43 (0.01)
TT_P0118	Cmr4	0.41 (<0.01)
TT_P0119	Cmr5	0.48 (<0.01)
TT_P0120	RAMP	0.38 (0.03)
TT_P0132	Cas3	0.22 (0.20)
TT_P0133	Cas4	1.14 (<0.01)
TT_P0134	Cas8C	0.80 (<0.01)
TT_P0135	Cas7	0.50 (<0.01)
TT_P0136	Cas4	0.48 (0.01)
TT_P0195	Cas2	1.42 (0.15)
TT_P0196	Cas1	0.52 (0.20)
TT_P0197	Cas4	0.34 (0.44)
TT_P0204	Cas6	0.73 (0.01)
TT_P0215	Cas1	0.16 (0.42)

Expression values are given as log_2 values of fold expression levels of the gene in strain HB27Δ*ago* relative to strain HB27, and *P* values (*t*-test) are indicated in brackets. Changes in expression are considered substantial if the log_2 value > 2 and $P < 0.02$ (Extended Data Fig. 2).

Extended Data Table 2 | Mass-spectrometry data of identified proteins after Strep(II)-tag affinity purification

a

Proteins with most abundant peptides

Protein ID	Name	Peptides	Sequence coverage (%)	Mol. Weight (kDa)	PEP	iBAQ
Q72G73	TT_C1975	31	42.8	76.8	1.64E-109	32756000
P61490	groL	16	28.4	57.9	1.09E-36	704330
Q746M7	TtAgo	14	19	76.7	1.95E-37	2642000
Q72JL4	TT_C0758	11	26.3	49.3	1.72E-41	2238900
Q72J15	TT_C0966	9	25.3	41.6	3.57E-29	1088200
Q72H68	TT_C1627	7	16.1	48.1	1.06E-19	340990
Q72HX7	TT_C1355	7	8.7	82.5	1.05E-19	272740
Q72GH6	TT_C1872	5	15.9	33.3	4.09E-17	612660
Q72K98	TT_C0549	5	16.3	35.9	3.04E-13	585590
Q72GW4	tuf1	5	12.3	44.8	1.97E-14	497870

b

Peptides matched against TtAgo

Sequence	Mass (Da)	Protein	PEP
AFGASGASLR	935.48248	TtAgo	0.00054319
AQETALALLR	1084.6241	TtAgo	5.97E-06
AVSKPADALR	1026.5822	TtAgo	0.0052086
EGIAYDLVSVR	1220.6401	TtAgo	0.0012876
EIASWIGR	930.49232	TtAgo	0.0065071
LADGLYVPLEDK	1331.6973	TtAgo	0.00097635
LGEEDPK	786.37595	TtAgo	0.013635
LGLGTPEAVR	1011.5713	TtAgo	0.00069792
LYPASGFAFPR	1224.6291	TtAgo	0.021229
MGQNYAYR	1001.4389	TtAgo	0.0050656
SVLSALAR	815.4865	TtAgo	0.0013518
TEVFLNR	877.46577	TtAgo	0.0013027
VAWVADPKDPR	1252.6564	TtAgo	0.023399
VYPVQGR	817.44464	TtAgo	0.033518

a, Only proteins of which five or more peptides were discovered are shown. The 'Peptides' column shows how many peptides are matches against a certain protein. iBAQ, intensity-based absolute quantification; PEP, posterior error probability. **b**, Peptides identified that match TtAgo sequence.

Extended Data Table 3 | TtAgo preferentially acquires ssDNA guides from plasmid DNA

DNA locus	Size	Copies per cell	Total DNA per cell	Reads aligned to DNA locus	Normalized reads*	Normalized reads* corrected for DNA per cell
***E. coli* K12 chromosome**	4.64 Mb	1	4.64 Mb	$23*10^6$	1	1
pWUR702	5.6 kb	20-40	0.17 Mb	$45*10^6$	2	54
pRARE	4.7 kb	10-12	52 kb	$2*10^6$	0.1	8.8

Estimated relative quantities of guides complementary to plasmid and chromosome DNA per cell.
* Reads are normalized against the number of reads mapped against the *E. coli* K12 chromosome.

Extended Data Table 4 | Strains and oligonucleotides

a

Strain	Abbreviations	Description	Source, reference
Thermus thermophilus HB27	HB27, wild type	ATCC BAA-163 / DSM 7039 / NBRC 101085	DSMZ
T. thermophilus HB27^{EC}	HB27^{EC}	*ago*::*ago*IS*Tth7* and multiple mutations, selected for enhanced competence	This study
T. thermophilus HB27 Δ*ago*	HB27Δ*ago*, knockout	Δ*ago*	This study
T. thermophilus HB27 Δ*ago*::*strep(II)-ago*	HB27Δ*ago*::^{s}*ago*	HB27Δ*ago* with *strep(II)-tag-ago* fusion and kanamycin marker insert	This study

b

Experiment	Primers	Sequence (5'-3')	Description, restriction sites
Genomic mutants	BG3524	AAAAAAAAGCTTCCTCAACGGGGAGGTTCCGGA	upstream region *ago* (fw), HindIII
	BG3525	AAAAAAGTCGACGCTCAGATTTGCATAGGAGCTGC	upstream region *ago* (rv), SalI
	BG3526	AAAAAAGTCGACATGGCAAGCTGGAGCCACCCG	*strep(II)-ago* (fw), SalI
	BG3527	AAAAAATCTAGACTAAACGAAGAAGAGCTTTTCCCG	*strep(II)-ago* (rv), XbaI
	BG3528	AAAAAATCTAGATGCCCAAGCGGGGCGGAACC	downstream region *ago* (fw), XbaI
	BG3529	AAAAAAGAATTCGGTCAATCCGCCCCGCTTCCA	downstream region *ago* (rv), EcoRI
	BG3563	GGCCGTCTAGACCCGGGAGTATAACAGAAACCTT	PslpA-Kan^{R}-stop (fw), XbaI
	BG3564	GCGCGTCTAGATCAAAATGGTATGCGTTTTGACAC	PslpA-Kan^{R}-stop (rv), XbaI
Expression vectors TtAgo	AgoFW	GCGCGCGGTACCAGATGAACCACCTTGGAAAAACGG	*T. thermophilus* HB8 *ago* (fw), KpnI
	AgoRV	GCGCGCGCGGCCGCGAATTCCTAAACGAAGAAGAGCTTTTCCC	*T. thermophilus* HB8 *ago* (rv), NotI
	BG4207	GCGCGCACATGTCAAGCTGGAGCCACCCGCAG	*strep(II)-ago* (fw), PciI
	BG4208	GCGCGCCCTAGGTTAATTAGTGGTGGTGATGG	*strep(II)-ago* (rv), AvrII
Site directed mutagenesis of *ago* gene	BG3454	GGCGGAGCTCGCCGTGGGCTTTGCCGCCGGCGGAAGGGAGTCCTTTCG	HB8 *ago* D478A (fw)
	BG3455	CGAAAGGACTCCCTTCCGCCGGCGGCAAAGCCCACGGCGAGCTCCGCC	HB8 *ago* D478A (rv)
	BG3456	CCCGGGTCCTCCTCCTTCGGGCCGGCCGCGTGCCCCAGGACGAG	HB8 *ago* D546A (fw)
	BG3457	CTCGTCCTGGGGCACGCGGCCGGCCCGAAGGAGGAGGACCCGGG	HB8 *ago* D546A (rv)
Guide sequencing	BG4409	GAGAGAGGATCCCGAATTGTGCA**GCT**GTCAATCAACC	5' Amplification primer, BamHI
	BG4436	GAGAGAGGATCCTTTTTTTTTTTTTTTTTTTTTTTTTVN	3' Poly-T primer with 'VN' anchor, BamHI
Target sequences	BG4262	GGCCATTTAATTAAATTAAAAGCTTGAATGCAATATTTATTTAAAAATTTATA CGAGGTAGTAGGTTGTATAGTATATTAAATTATTTAAATATAAAG	Low GC-content (17%) target oligonucleotide 'FW-target'
	BG4263	TCGACTTTATATTTAAATAATTTAATATACTATACAACCTACTACCTCGTATA AATTTTTAAATAAATATTGCATTCAAGCTTTTAATTTAATTAAAT	Low GC-content (17%) target oligonucleotide 'RV-target'
	BG4264	GGCCAGGTCCACCATGCGTAAGCTTGAATGCCGGCCAGCCCAAGGGCTC TGCACGAGGTAGTAGGTTGTATAGTTGCTGGCAGGCGTAGGTCTAAGCG	High GC-content (59%) target oligonucleotide 'FW-target'
	BG4265	TCGACGCTTAGACCTACGCCTGCCAGCAACTATACAACCTACTACCTCGTG CAGAGCCCTTGGGCTGGCCGGCATTCAAGCTTACGCATGGTGGACCT	High GC-content (59%) target oligonucleotide 'RV-target'
	BG3467	CTAGACGAGGTAGTAGGTTGTATAGTA	Target sequence insert, XbaI, HindIII
	BG3468	AGCTTACTATACAACCTACTACCTCGT	Target sequence insert, XbaI, HindIII
siDNA and siRNA sequences	BG3466	P-TGAGGTAGTAGGTTGTATAGT	FW-guide, based on *let-7* miRNA
	BG4017	P-TTATACAACCTACTACCTCGT	RV-guide, based on reverse complement of *let-7* miRNA
	BG4500	P-AGAGGTAGTAGGTTGTATAGT	FW-guide, based on *let-7* miRNA, 5'-end deoxyadenosine
	BG4501	P-GGAGGTAGTAGGTTGTATAGT	FW-guide, based on *let-7* miRNA, 5'-end deoxyguanosine
	BG4502	P-CGAGGTAGTAGGTTGTATAGT	FW-guide, based on *let-7* miRNA, 5'-end deoxycytidine
	BG4503	P-TGAGGTAGTAGGTTGTATAGT	FW-guide, based on *let-7* miRNA, 5'-end deoxythymidine
	BG4508	P-UGAGGUAGUAGGUUGUAUAGU	FW-guide, based on *let-7* miRNA

a, *T. thermophilus* strains used in this study. **b**, Oligonucleotides used in this study; restriction sites are underlined.

Extended Data Table 5 | Plasmids

Plasmid	Description	Restriction sites used	Primers	Source, reference
pRARE	*E. coli* Rosetta (DE3) plasmid, encodes rare tRNAs, Cam^R			Novagen
pET-52b(+)	T7 RNA polymerase based expression vector, Amp^R			Novagen
pWUR627	*T. thermophilus* HB8 *ago* with N-term. *strep(II)-tag* in pET-52b(+) expression vector for TtAgo	KpnI NotI	AgoFW AgoRV	This study
pWUR641	pWUR627, *ago* active site residue substituted (D546A)	-	BG3456 BG3457	This study
pWUR642	pWUR641, *ago* active site residue substituted (D478A) Expression vector for TtAgoDM(D478A,D546A)	-	BG3454 BG3455	This study
pCDF-1b	T7 RNA polymerase based expression vector, Sm^R			Novagen
pWUR702	*strep(II)-ago* insert from pWUR627 inserted in pCDF-1b Expression vector for TtAgo	AvrII NcoI	BG4207 BG4208	This study
pWUR703	*strep(II)-agodm*(D478A,D546A) insert from pWUR642 inserted in pCDF-1b Expression vector for TtAgoDM(D478A,D546A)	AvrII NcoI	BG4207 BG4208	This study
pUC18	Amp^R			Thermo scientific
pUC19	Amp^R			Thermo scientific
pWUR673	2.4kb downstream sequence of *ago* inserted in pUC18	XbaI EcoRI	BG3528 BG3529	This study
pWUR674	1kb upstream sequence of *ago* inserted in pWUR673	HindIII SalI	BG3524 BG3525	This study
pWUR675	*ago* with N-terminal *strep(II)-tag* inserted in pWUR674	SalI XbaI	BG3526 BG3527	This study
pWUR676	Kan^R marker with pSLPa promoter inserted in pWUR675	XbaI XbaI	BG3563 BG3564	This study
pK18	Recombination vector			27
pWUR701	Insert from pWUR674 transferred to pK18	HindIII EcoRI		This study
pMHPnqosGFP	*E. coli* / *T. thermophilus* shuttle vector, Hyg^R, sGFP under control of Pnqo promoter			30
pMKPnqosGFP	*E. coli* / *T. thermophilus* shuttle vector, Kan^R, sGFP under control of Pnqo promoter			30
pMK184	*E. coli* / *T. thermophilus* shuttle vector, Kan^R			31
pFU98	pSC101 ori, rbs-luxCDABE, Cam^R			29
pWUR677	pFU98, Cam^R marker replaced by Hyg^R marker	SacI NheI	BG3870 BG3871	This study
pWUR704	pWUR677, rbs-luxCDABE replaced by annealed BG4262-BG4263	NotI SalI	BG4262 BG4263	This study
pWUR705	pWUR677, rbs-luxCDABE replaced by annealed BG4264-BG4265	NotI SalI	BG4264 BG4265	This study
pWUR708	pWUR677, rbs-luxCDABE replaced by annealed BG3467-3468 insert	XbaI HindIII	BG3467 BG3468	This study

List of plasmids and dsDNA fragments used in this study. References 27, 29, 30 and 31 are cited in this table.